Am J Cancer Res 2021;11(6):3123-3134
www.ajcr.us /ISSN:2156-6976/ajcr0130339

Original Article

A novel CT-based radiomic nomogram for predicting the recurrence and metastasis of gastric stromal tumors

Weiqun Ao[1], Guohua Cheng[2], Bin Lin[3], Rong Yang[4], Xuebin Liu[4], Sheng Zhou[5], Wenqi Wang[5], Zhaoxing Fang[2], Fengjuan Tian[6], Guangzhao Yang[1*], Jian Wang[1*]

[1]Department of Radiology, Tongde Hospital of Zhejiang Province, Hangzhou, Zhejiang, China; [2]Jianpei Technology, Hangzhou, Zhejiang, China; [3]Department of Radiology, Second Affiliated Hospital, Zhejiang University School of Medicine, Hangzhou, Zhejiang, China; [4]Department of Radiology, First Affiliated Hospital, Zhejiang University School of Medicine, Hangzhou, Zhejiang, China; [5]Department of Radiology, Gansu Provincial Hospital of Traditional Chinese Medicine, Lanzhou, Gansu, China; [6]Department of Radiology, Sir Run Run Shaw Hospital, Zhejiang University School of Medicine, Hangzhou, Zhejiang, China. [*]Equal contributors.

Received January 18, 2021; Accepted April 17, 2021; Epub June 15, 2021; Published June 30, 2021

Abstract: Our study aimed to explore the value of applying the CT-based radiomic nomogram for predicting recurrence and/or metastasis (RM) of gastric stromal tumors (GSTs). During the past ten years, a total of 236 patients with GST were analyzed retrospectively. According to the postoperative follow-up classification, the patients were divided into two groups, namely non-recurrence/metastasis group (non-RM) and RM group. All the cases were randomly divided into primary cohort and validation cohort according to the ratio of 7:3. Standardized CT images were segmented by radiologists using ITK-SNAP software manually. Texture features were extracted from all segmented lesions, then radiomic features were selected and the radiomic nomogram was built using least absolute shrinkage and selection operator (LASSO) method. The clinical features with the greatest correlation with RM of GST were selected by univariate analysis, and used as parameters to build the clinical feature model. Eventually, model of radiomic and clinical features were fitted to construct the clinical + radiomic feature model. The performance of each model was evaluated by the area under receiver operating characteristic (ROC) curve (AUC). A total of 1223 features were extracted from all the segmentation regions of each case, and features were selected via the least absolute shrinkage and LASSO binary logistic regression model. After deletion of redundant features, four key features were obtained, which were used as the parameters to build a radiomic signature. The AUCs of radiomic nomogram in primary cohort and validation cohort were 0.816 and 0.946, respectively. The AUCs of clinical + radiomic feature model in primary cohort and validation cohort were 0.833 and 0.937, respectively. Using DeLong test, the differences of AUC values between radiomic nomogram and clinical + radiomic feature model in primary cohort (P = 0.840) and validation cohort (P = 0.857) were not statistically significant. To sum up, CT-based radiomic nomogram is of great potential in predicting the RM of GST non-invasively before operation.

Keywords: Computed tomography, radiomics, gastric stromal tumors, recurrence, metastasis

Introduction

Gastrointestinal stromal tumor (GIST) is one of the most common primary mesenchymal tumors in gastrointestinal tract, and accounts for <1% of all gastrointestinal tumors [1]. The biological behavior of GIST varies widely, thus it is of great importance to accurately and preoperatively predict the RM of GIST as to guide adjuvant therapy and predict disease prognosis [2]. GISTs are the most common type of sarcoma, which are mostly malignant in nature. Most GISTs are localized (79.4%), but approximately 11.4% of all cases have regional/distant metastases at the time of presentation. Up to 30% of the GISTs have poor prognosis due to factors including tumor size >5 cm, lobulated contour, presence of mesenteric fat infiltration, ulceration, heterogeneous enhancement, regional lymphadenopathy or an exophytic growth pattern on CT [3].

The National Institutes of Health (NIH) 2008 criteria is the most widely used guideline for assessing the relative risk of GIST [4]. Based on tumor size, location, tumor rupture and mitosis

count, GIST can be classified into four risk categories, namely very low-, low-, intermediate-, and high-risk tumors [4]. With the increase of risk and malignancy, the outcome of GIST patients deteriorates dramatically [5]. A modification to the NIH criteria has been proposed that tumor site and tumor rupture should be incorporated [6] to optimize the performance.

GISTs can be found in any site along the gastrointestinal tract, but they most commonly arise from the stomach (60%), followed by the small intestine (30%), duodenum (5%), colon (4%), and appendix or esophagus (1%) [7]. Clinical presentation varies widely depending on the tumor size and location. According to these guidelines, gastric GISTs that are 2 cm or smaller and with a mitotic index of 5 or less per 50 HPF can be regarded as essentially benign, while gastric lesions larger than 2 cm and with the same mitotic index have a higher risk for recurrence [8]. Recurrence after primary local treatment is mainly intra-abdominal. The most common site of metastasis is in the liver, whereas metastases in bones, peripheral skin, soft-tissue, lung and lymph node are less common [8].

Radiomics is a new quantitative imaging method that allows thorough analysis of medical images and has attracted increasing attention in the field of medicine in recent years. Radiomics extracts numerous numerical features from medical images to facilitate clinical decision-making [9]. It provides a new angle for individualized diagnosis, differential diagnosis, prediction of malignancy or metastasis potential, treatment, curative effect evaluation of tumor and prediction of tumor prognosis [10-12].

Previous studies have demonstrated that the RM of gastrointestinal neoplasms were related to some imaging features. However, these studies showed low diagnostic efficiency and controversial results [13, 14]. The underlying explanation might be that the previous analyses were only based on quantifiable parameters derived from imaging pictures or imaging features extracted by naked eyes that lacked a proper validation. Although interpretation by naked eyes provides valuable feature information, some microcosmic imaging features related to clinical outcomes may be lost due to the limited image contrast detected by naked eyes [15], and the results are easily influenced by different individuals. In recent years, some studies have identified radiomics as a superior tool for predicting the malignancy of gastrointestinal neoplasms. CT-based radiomics has shown good performance in the investigation of gastrointestinal tumors, especially in gastric cancer [16, 17]. Some researches applying CT-based radiomics [18, 19] have been done in GIST and showed satisfactory results. However, different locations of GIST might affect the prognosis. Gastric GISTs have a better prognosis than non-gastric GISTs with the same size and mitotic count [1]. To the best of our knowledge, whether CT-based radiomics approach is superior than other methods for predicting RM of gastric stromal tumors (GSTs) has not been evaluated. Therefore, by adopting artificial intelligence (AI) technology to extract different texture features in GST, we aimed to explore the value of CT-based radiomic nomogram in predicting the RM of GST.

Materials and methods

Patients

This retrospective study was approved by the institutional review board of Tongde Hospital of Zhejiang Province. The requirement for written informed consent was waived because of the retrospective study design. A total of 236 patients with GST were enrolled from January 2009 to July 2019 (121 males and 115 females, mean age: 59 years, range: 45-75 years). The flow chart showed the enrollment of patients (**Figure 1**). Inclusion criteria: 1) the follow-up time was more than 1 year; 2) the patient had complete medical history and imaging data; 3) contrast-enhanced examinations were done within the 30-day period before treatment; 4) no diagnostic treatment was performed before CT examination. Exclusion criteria: 1) confirmative pathological data were missing; 2) the follow-up time was less than 1 year; 3) incomplete or missing clinical/CT data; 4) the maximum diameter of the tumor was less than 1 cm, which was difficult to delineate. All the cases were randomly divided into primary cohort (cases for training) and validation cohort (cases for testing) according to the ratio of 7:3.

CT examination

All patients underwent CT examinations on 16-MDCT (SOMATOM Emotion16, SIEMENS, Germany), 64-MDCT (Definition AS, SIEMENS,

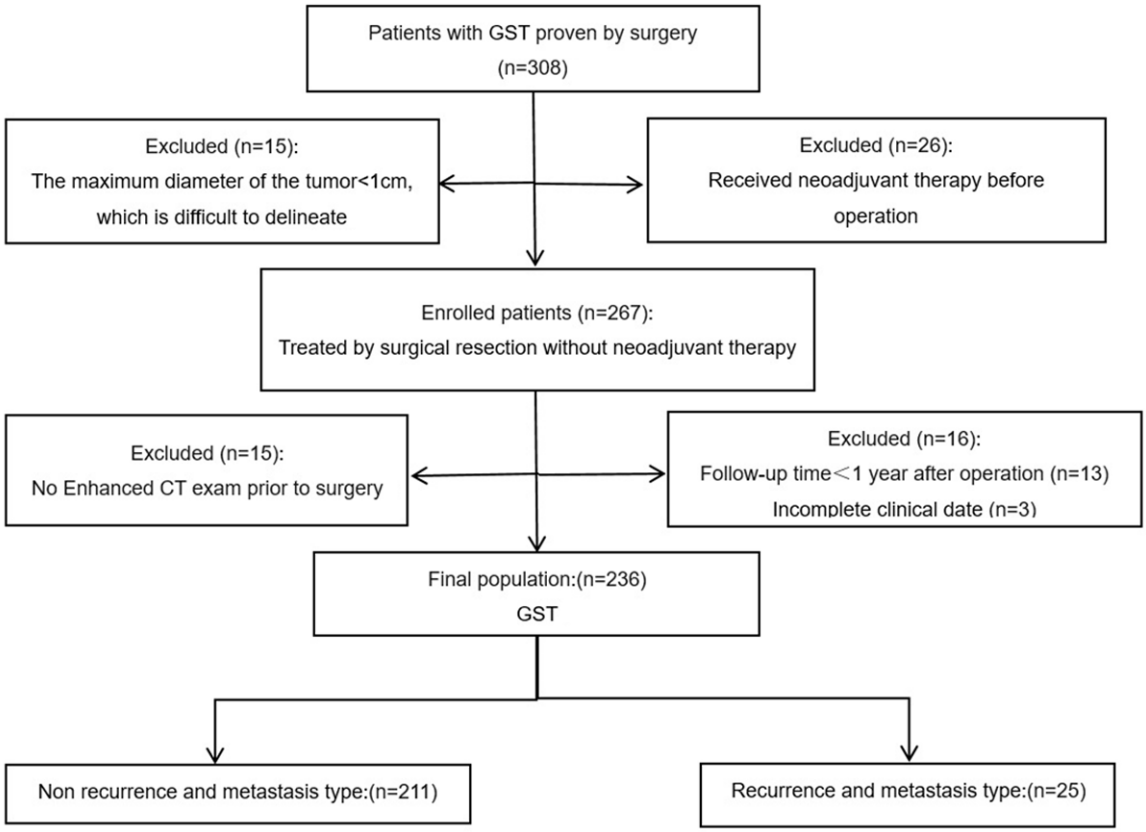

Figure 1. Flow diagram of enrolled and excluded patients.

Germany) or 64-MDCT (Optima CT680, GE, USA) scanners. They had plain and enhanced CT scan before operation. After fasting for at least 6 hours, each patient ingested about 600-1000 ml of water more than 15 minutes before scanning. MSCT dual-phase enhanced images were obtained during the arterial phase (33-35 s after initiation of the injection) and portal venous phase (60-65 s after initiation of the injection). The parameters for both plain and enhanced CT examinations were: tube voltage, 120-130 kV; tube current, 180~210 mAs; slice thickness, 1.5 mm.

Image analysis

MSCT image data were retrospectively reviewed by two radiologists (W.A. and J.W.), both of whom had more than 15 years of experience in abdominal imaging. The radiologists were blinded to the clinical and pathological data of all the patients. Discrepancies between the readers were resolved by consensus after joint re-evaluation of the images. The CT examinations were reviewed in random order, with a time interval of at least one month.

The following CT features were evaluated on the picture archiving and communication systems workstation (PACS): contour (regular or irregular), necrosis, calcification, presence/absence of intratumoral vessel, growth pattern (endoluminal, exophytic, or mixed), location, RM (lymph node, liver or peritoneum). The largest dimension of the lesion was selected when measuring the maximum diameter of the tumor interface (MaxDT) and minimum diameter of the tumor interface (MinDT) of the lesion. Enhancement pattern of GST was also evaluated. The CT value (HU) was also measured by drawing the region of interest (ROI) on the tumor in the same axial image. ROI was drawn over solid portion of mass excluding vessels, calcification, and the necrotic parts. The CT values of tumor were measured on non-contrast phase, arterial phase, and portal venous phase, which were recorded as CTU, CTA and CTV respectively. Absolute enhancement was measured.

Tumor absolute enhancement on arterial and portal venous phase: DEAP = CTA - CTU, DEPP = CTV - CTU.

Image segmentation and radiomics feature extraction

All CT images were retrospectively interpreted by two radiologists (B.L. and J.W.) who had 8-year (B.L.) and 15-year (J.W.) experience in gastrointestinal radiology. All venous phase CT images were downloaded from the PACS (picture archiving and communication system) and uploaded into the open-source ITK-SNAP software (www.itk-snap.org). Each ROI was manually drawn along the margin and on every slice of the tumor in portal venous phase. The segmentation procedure was performed by an abdominal radiologist (B.L.) and were verified by a senior radiologist with 15 years of experience in gastrointestinal radiology (J.W.).

Pyromics version 3.0.0 (http://www.radiomics.io/pyradiomics.html) was used to extract the radiomic characteristics from lesions. The most useful predictive features were selected by using least absolute shrinkage and selection operator (LASSO) method. Briefly, the optimized hyperparameter λ was firstly determined by using 10-fold cross validation with binomial deviance as criterion. Then the features with non-zero coefficient were selected based on the determined optimal λ. Finally, LASSO logistic regression was conducted to construct the radiomics model and a radiomics score (Rad-score) was calculated for each patient via a linear combination of selected and weighted features by their corresponding coefficients. The clinical features with the greatest correlation with RM of GST were screened by univariate analyses, and were used as parameters to construct the clinical feature model. Finally, radiomic and clinical features were fitted to construct the clinical + radiomic feature model. The performance of each model was evaluated by the area under ROC curve (AUC) (**Figure 2**).

Statistical analysis

R software (version 3.6.3; http://www.Rproject.org) was used for all statistical analyses. The 'caret' package was used to obtain the accuracy, sensitivity and specificity of the model. 'pROC' package was used to perform ROC analysis. DeLong test was used to compare the AUC of radiomic nomogram and clinical + radiomic feature model in primary and validation cohort. Two-sided P<0.05 indicated statistical significance.

Results

Radiomics features selection and radiomics model construction

A total of 1223 features were extracted from all the segmentation regions of the same case, and features including 18 first-order statistical properties, 12 shapes, 75 textures, 372 wavelets and other 508 filtering features were selected via the least absolute shrinkage and LASSO binary logistic regression model. After reduction of the redundant features, four key features were obtained, including original shape Sphericity (OSS), wavelet.HHL glcm Maximum Probability (GLCM), wavelet.LLL firstorder Median (WLFM), and logarithm glszm large area low gray level emphasis (GLSZM) which were used as the parameters of radiomic signature to build radiomic nomogram. The four selected radiomics features and their corresponding coefficients are shown in **Table 1**.

Clinical and radiomics model construction

The primary cohort included 165 patients and the validation group included 71 patients. The main clinical data of patients in primary and validation groups were summarized in **Table 2**. These characteristics were analyzed by univariate analysis and P<0.05 was considered statistically significant. In addition to the radiomic features, the clinical data (termed "clinical feature" later in this article) were also collected. As a result, nine clinical features were obtained (**Figure 3**): Risk level, contour, necrosis, intratumoral vessel, tumor volume, MaxDT, MinDT, cyst volume and Cyst/Tumor volume, all of which were significantly different between severe and non-RM types of GST by univariate logistic regression analysis. There were no significant differences in age, gender, degree of enhancement, symptom and underlying disease in risk assessment of GST between the two groups. The univariate logistic results are also shown in **Table 2**. The nine significant clinical features were combined with rad-score to build the stepwise logistic regression. The significant features and their corresponding coefficients are shown in **Table 3**.

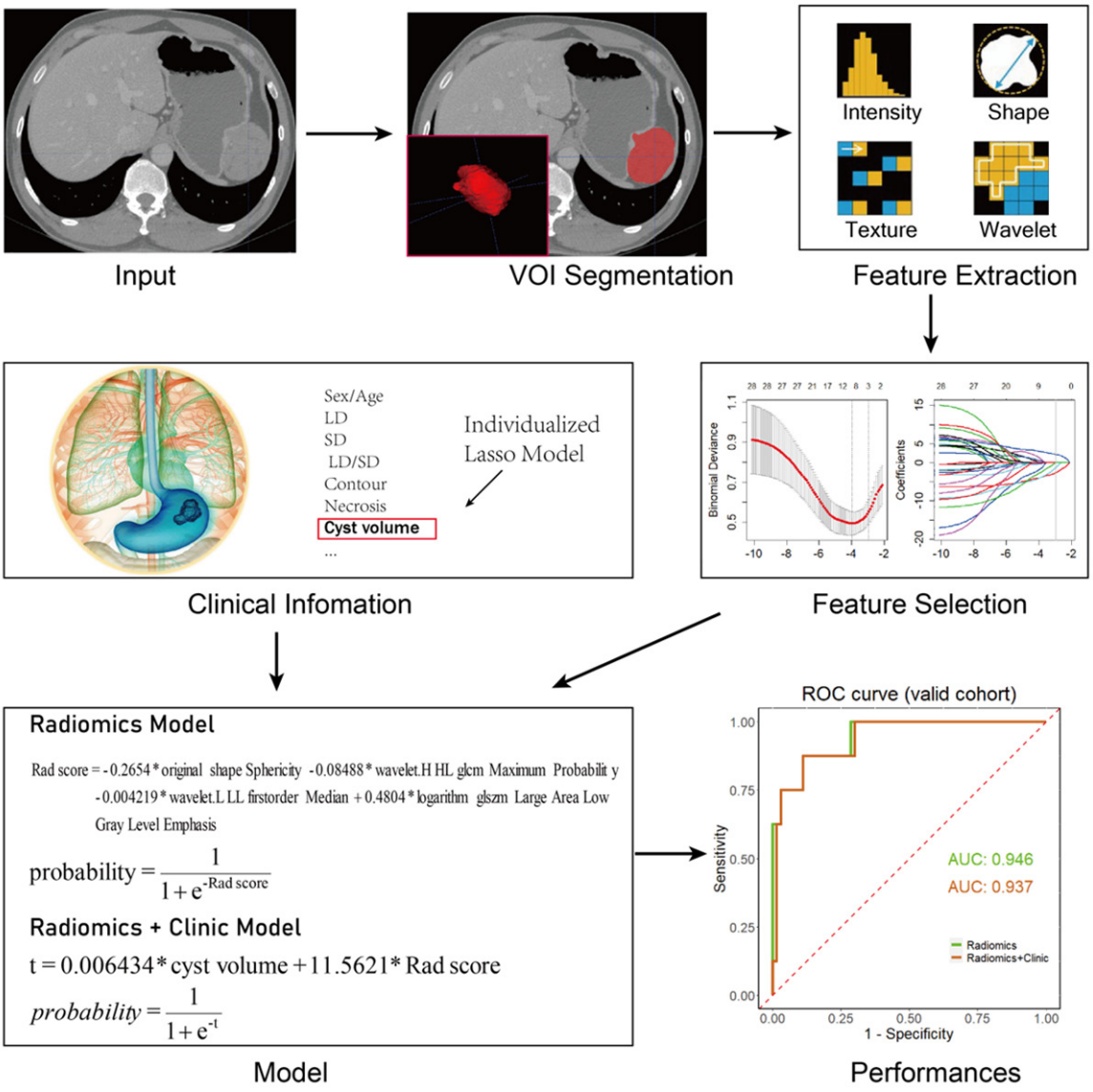

Figure 2. Flow chart of radiomic nomogram: Image segmentation and radiomics feature extraction of GST. Feature selection via LASSO binary logistic regression model. The parameter (λ) was screened by using 10-fold cross-validation method and parameter (λ) between two dotted lines was the optimal value by using the minimum criteria and the 1 standard error of the minimum criteria (the 1-SE criteria). LASSO coefficient profiles of the 28 radiological features. A coefficient profile plot was conducted against the log (λ) sequence. λ value of 0.019, with log (λ), -3.96 was selected (1-SE criteria) based on 10-fold cross-validation. Vertical line was drawn at the value selected, where resulted in 4 non-zero coefficients. Finally, radiomic and clinical features were fitted to construct the radiomic model. The performance of each model was evaluated by the area under ROC curve.

Performance and evaluation of models in primary cohort and validation cohort

The same logistic regression model as established in the primary cohort was used on the validation cohort. Finally, ROC analysis was used to evaluate the performance of the logistic model. Accuracy, sensitivity and specificity were calculated in both primary cohort and validation cohort (**Table 4**). ROC analyses for the primary cohort and validation cohort were shown in **Figure 4**. The AUC, accuracy, sensitivity and specificity of radiomic nomogram were 0.816, 77.0%, 76.5% and 77.0% respectively in the primary cohort, while they were 0.946, 88.7%, 87.5% and 88.9% respectively in the validation cohort. Diagnostic efficiency in predicting RM of GST in the validation cohort was

Table 1. The selected radiomic features and relevant coefficients in radiomics model

Radiomic features	Regression coefficient
original shape Sphericity	-0.2654
wavelet.HHL glcm Maximum Probability	-0.08488
wavelet.LLL firstorder Median	-0.004219
logarithm glszm large area low gray level emphasis	0.4804

Note: The most useful predictive features were selected by using the least absolute shrinkage and selection operator (LASSO) method. Briefly, the optimized hyperparameter λ was first determined by using 10-fold cross validation with binomial deviance as criterion. Then the features with non-zero coefficient were selected based on the determined optimal λ. Finally, LASSO logistic regression was conducted to construct the radiomics model and a radiomics score (Rad-score) was calculated for each patient via a linear combination of selected and weighted features by their corresponding coefficients. The equations of the Rad-score and the probability of RM in clinical and radiomics model are: Radscore=-0.2654*original shape Sphericity-0.08488*wavelet.HHL glcm Maximum Probability-0.004219*wavelet.LLL firstorder Median+o.4804*logarithmglszm Large Area Low Gray Level Emphasis

$$\text{probability} = \frac{1}{1+e^{-\text{Rad\_score}}}$$

higher than that in the primary cohort. The AUC, accuracy, sensitivity and specificity of clinical + radiomic feature model were 0.833, 77.0%, 76.5% and 77.0% respectively in the primary cohort, while they were 0.937, 88.7%, 87.5% and 88.9% respectively in the validation cohort. The diagnostic efficiency of clinical + radiomic feature model in predicting RM of GST in the validation cohort was significantly higher than that in the primary cohort. Using DeLong test, the differences of AUCs between radiomic nomogram and clinical + radiomic feature model in primary cohort (*p*-value = 0.840) and validation cohort (*p*-value = 0.857) were not statistically significant (**Table 4**).

Discussion

Previous researches [15, 20, 21] that preoperatively predicted the RM of gastrointestinal tumors mainly focused on the morphological features. They used tumor location, shape, size, contour, necrosis, enhancement change and growth pattern to distinguish different risk levels of gastrointestinal tumors. These studies showed that imaging morphologic features can be used to assess the metastatic risk of gastrointestinal tumors. However, their results were largely dependent on the experience of doctors and influenced by personal interpretation greatly. Meanwhile, assessment results varied among different doctors and lacked reproducibility. In comparison, radiomics is a promising tool by which we can extract high-dimensional mineable features from medical images using a series of data-characterization algorithms. Thus CT-based radiomics analysis attracts increasing attention for the preoperative evaluation of GIST. Some studies [15, 22] showed that CT-based radiomics nomogram was useful in diagnosing gastrointestinal tumors and in differentiating benign and malignant gastrointestinal tumors.

Radiomics allows quantifying lesion heterogeneity and extracting additional quantitative data that cannot be evaluated by human eyes [23]. In our study, a total of 1223 two-dimensional features were extracted from each ROI. After reduction of redundant features, four selected radiomics features were used as the parameters to build a radiomic signature. These features not only represent different characteristics of the lesions, but also reflect the heterogeneity of the tumor. OSS represents the morphological characteristics of tumor. GLCM Probability is a texture feature, which is described as a combination of different gray values, distances and angles of the images. This study was based on the GLCM feature of wavelet transform. Texture features based on wavelet transform can be used to predict the early metastasis of tumor. WLFM describes the intensity of voxel distribution in the ROI. The prediction model in our group was based on the primary cohort and tested in the validation cohort. So the prediction model has shown high reliability and strength. GLSZM represents the low gray value distribution of images, the higher the value, the higher the concentration of low gray value in the image. Our results indicate that CT-based radiomic nomogram has certain potential in non-invasively predicting the RM of GST before operation.

Besides the radiomic features, the clinical features were also collected. We found that nine clinical features, including risk level, contour, necrosis, intratumoral vessel, tumor volume, MaxDT, MinDT, cyst volume and Cyst/Tumor volume were significantly different between RM and non-RM types of GST by univariate logistic

Table 2. Clinical characteristics of patients in the primary and validation cohorts

Characteristic	Primary Cohort (n = 165)		*P*	Validation Cohort (n = 71)		*P*
	Non-RM type (n = 148)	RM type (n = 17)		Non-RM type (n = 63)	RM type (n = 8)	
Sex (Male, %)	78 (52.7)	9 (52.9)	0.9852	30 (47.6)	4 (50.0)	0.9007
Age	59.4±11.32	54.8±10.85	0.1079	60.4±9.57	64.5±17.29	0.3102
Risk level			<0.001			<0.001
Very low	28	1		7	0	
Low	60	1		21	0	
Intermediate	42	5		26	0	
High	18	10		9	8	
CTU	34.4±7.98	31.4±5.96	0.1426	33.2±6.92	33.1±4.11	0.9832
CTA	56.0±13.98	50.9±13.49	0.1512	52.3±13.94	54.5±11.88	0.6725
CTP	70.9±17.52	67.3±16.85	0.4232	66.5±18.58	66.1±13.01	0.9475
DEAP	21.7±13.08	19.5±12.95	0.5115	19.1±12.19	21.4±11.95	0.6249
DEPP	36.6±18.11	35.9±17.84	0.8894	33.3±18.11	32.9±11.02	0.9522
Location			0.6151			0.5972
Cardia	7 (4.7)	1 (5.9)		1 (1.6)	0	
Fundus	49 (33.1)	7 (41.2)	1	17 (27.0)	2 (25.0)	0.7502
Body	79 (53.4)	9 (52.9)	0.8409	34 (54.0)	3 (37.5)	0.8039
Antrum	13 (8.8)	0	0.3647	11 (17.4)	3 (37.5)	0.5212
Contour			0.0012			0.0147
Round	57 (38.5)	2 (11.8)		20 (31.8)	0	
Oval	44 (29.7)	2 (11.8)	0.8687	14 (22.2)	0	1
Irregular	47 (31.8)	13 (76.4)	<0.001	29 (46.0)	8 (100.0)	0.0125
Growth pattern			0.0886			0.0016
Endophtic	64 (43.2)	3 (17.6)		20 (31.8)	0	
Exophytic	62 (41.9)	9 (52.9)	0.1132	31 (49.2)	2 (25.0)	0.4695
Mixed	22 (14.9)	5 (29.4)	0.0432	12 (19.0)	6 (75.0)	<0.001
Necrosis	55 (37.2)	14 (82.4)	<0.001	28 (44.4)	8 (100.0)	0.0027
Calcification	20 (13.5)	5 (29.4)	0.0843	13 (20.6)	3 (37.5)	0.2888
Surface unceration	28 (18.9)	6 (35.3)	0.1153	13 (20.6)	4 (50.0)	0.0683
Intratumoral vessel	14 (9.5)	7 (41.2)	<0.001	4 (6.3)	3 (37.5)	0.0049
Symptom			0.3824			0.2026
No	48 (32.4)	8 (47.1)		28 (44.4)	1 (12.5)	
Yes[1]	78 (52.7)	6 (35.3)	0.1765	22 (34.9)	5 (62.5)	0.0786
Yes[2]	22 (14.9)	3 (17.6)	0.7558	13 (20.6)	2 (25.0)	0.3282
Underlying disease			0.5992			0.2778
0	65 (43.9)	10 (58.8)		26 (41.3)	4 (50.0)	
1	29 (19.6)	3 (17.6)	0.5409	17 (27.0)	4 (50.0)	0.5277
2	30 (20.3)	3 (17.6)	0.5078	11 (17.4)	0	0.236
≥3	24 (16.2)	1 (5.9)	0.1884	9 (14.3)	0	0.2714
Tumor marker			0.1902			0.7508
0	102 (68.9)	16 (94.1)		44 (69.8)	7 (87.5)	
1	39 (26.4)	1 (5.9)	0.0479	14 (22.2)	1 (12.5)	0.4589
2	3 (2.0)	0	0.4455	1 (1.6)	0	0.6748
≥3	4 (2.7)	0	0.3804	4 (6.3)	0	0.4155
Tumor volume	62.7±201.95	581.9±1163.80	<0.001	80.8±282.25	788.8±1067.62	<0.001
MAT	2.22±3.43	11.7±20.99	<0.001	3.2±4.92	14.3±13.37	<0.001

MaxDT	41.4±28.29	89.0±64.32	<0.001	45.9±26.99	119.4±60.15	<0.001
MinDT	31.4±18.37	57.7±32.44	<0.001	36.3±20.01	73.2±34.07	<0.001
Cyst volume	7.0±31.22	248.8±768.41	<0.001	16.1±97.90	226.2±346.41	<0.001
Cyst/Tumor volume	0.076±0.140	0.125±0.19	0.1931	0.090±0.1297	0.192±0.177	0.0491

Note: Besides the radiomic features, the clinical features were also collected. Nine clinical features were significant difference between RM and non-RM type of GST disease in univariate logistic regression analysis. RM = recurrence and metastasis; CTU/CTA/CTP = the CT attenuation value of unenhancement phase/arterial phase/portal venous phase; DEAP = the CT attenuation value of arterial phase-unenhanced phase; DEPP = the CT attenuation value of portal venous phase-unenhanced phase; Yes[1] = no hematemesis and melena; Yes[2] = with or without hematemesis and/or melena. MAT = Maximum area of the tumor; MaxDT/MinDT = maximum/minimum diameter of the tumor interface; Underlying disease: hypertension, diabetes, hyperlipidemia and diseases of vital tissues and organs; Tumor marker: ferritin, CA125, CA153, CA242, CA199, CEA, AFP.

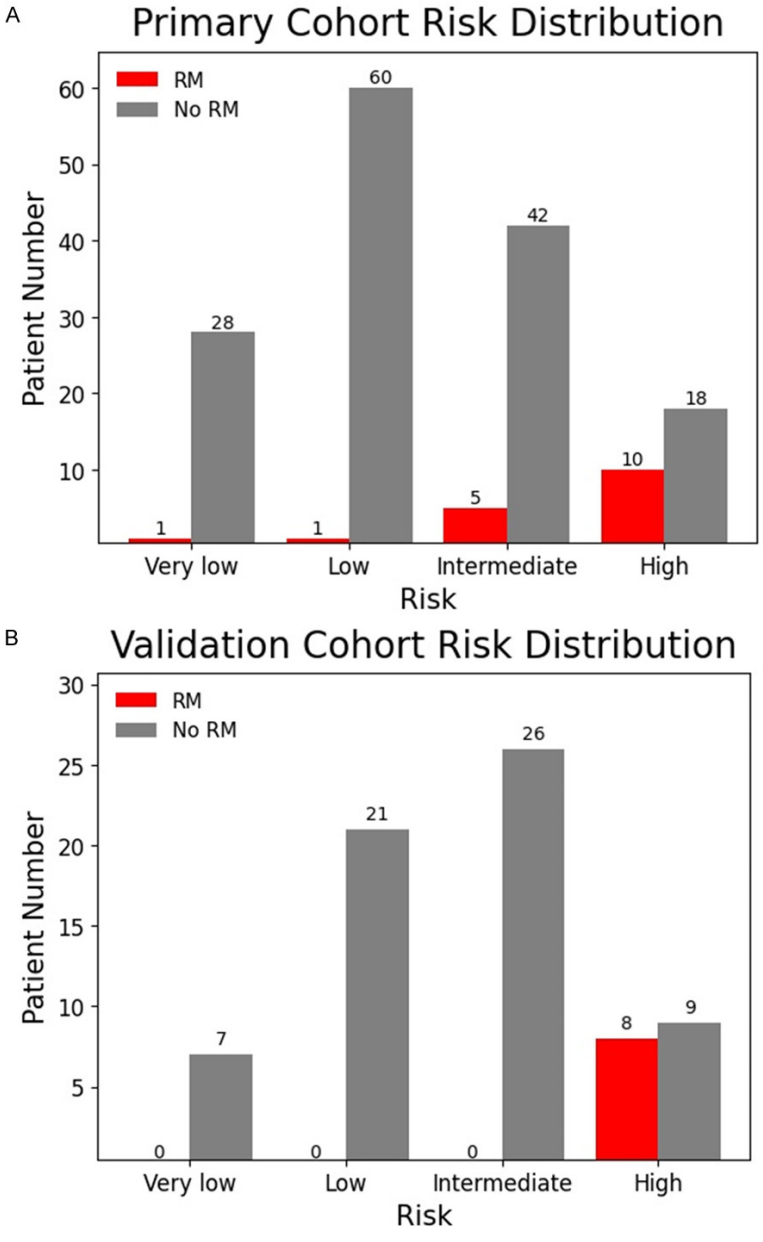

Figure 3. Risk distribution of GST patients in Primary (A) and validation (B) cohorts. RM patients are mostly distributed in the intermediate and high-risk groups of GST in primary cohort, and RM patients were all distributed in the high-risk group of GST in validation cohort. RM: recurrence and metastasis.

regression analysis. By adding the clinical feature, we constructed the clinical + radiomic feature model for predicting RM of GST. Some studies [18, 24] showed that tumor size and hemorrhage provided important evidence for poor prognosis of GIST. Tumor size is a significant factor for evaluating the biological behavior of GIST. Nevertheless, evaluating the malignancy of GIST merely by tumor size is insufficient because some small GIST may be aggressive and have a poor prognosis. Xu et al. [25] established and validated a multi-class scoring system for preoperative GIST risk stratifications based on CT features and found that five CT features, including tumor size, intratumoral enlarged vessels, ill-defined margin, heterogeneous enhancement pattern, and growth pattern were associated with the different levels of intratumoral heterogeneity and malignant potential of GIST. These results were consistent with our study. Our results showed that morphology of tumor such as size, contour and tumor volume were significant factors for predicting RM of GST ($P< 0.05$). Meanwhile, our study also revealed that internal structures of the lesions such as necrosis and intratumoral vessel were significant fac-

Table 3. The selected radiomic features and relevant coefficients in radiomics model

Features	Regression coefficient	*p*-value
Intercept	-3.8998	<0.0001
Cyst volume	0.006434	0.0404
Rad score	11.5621	0.00133

Note: The nine significant clinical features were combined with rad-score to build the stepwise logistic regression. The equation of the probability of RM in clinical and radiomics model is t=0.006434*cyst volume+11.5621*Rad score probability $= \frac{1}{1 + e^{-t}}$

tors for predicting RM of GST (P<0.05). These two CT features might reflect the high level of intratumoral heterogeneity associated with RM of GST, which has not been mentioned in other literature. However, age, gender and CT enhancement difference had no significant effect on predicting RM of GST (P>0.05). However, Zheng et al. [26] found that high-risk GIST presented significantly greater volume (P<0.01) and faster enhancement (P<0.05) than that of GIST in the low-risk group.

The clinical and CT data of 236 patients with GST were collected in our study. To our knowledge, the sample size of the current study is the largest among CT-based radiomic nomogram studies, which assures the stability of prediction model. Patients were randomly divided into primary and validation cohort with the proportion of 7:3, so as to assure the randomicity of the measured sample. The method reduced statistical deflection of amplitude. A large number and various types of radiomic features were extracted from all the segmentation regions in our study. They reflected high-throughput extraction of the radiomic nomogram. In other studies, Chen et al. [18] developed and evaluated a CT-based radiomics nomogram from 222 patients for differentiating the malignancy risk of GIST. The results showed that the radiomics model could differentiate low- and high-malignant-potential GIST with satisfactory accuracy compared with subjective CT findings and clinical indexes. CT radiomics nomogram predicted the malignant potential of GIST with excellent accuracy. Zhang et al. [5] retrospectively analyzed 366 patients with GIST and found that CT-based radiomics signature showed good diagnostic accuracy in distinguishing nonadvanced GIST from advanced ones. Based on postoperative pathology, Wang et al. [27] categorized 333 patients with GIST by malignant potential and mitotic count before construction of predictive CT-based radiomic models, which showed a good predictive performance for preoperative risk stratification of GIST and could be used to accurately differentiate high- from low-mitotic count GIST.

Our study demonstrated that the diagnostic efficiency in predicting RM of GST in validation cohort was better than that in primary cohort. After addition of the clinical feature, the diagnostic efficiency of clinical + radiomic feature model in predicting RM of GST in the validation cohort was also better than that in the primary cohort. In general, the diagnostic performance was slightly worse in the primary cohort than that in the validation cohort. However, there were discrepancies among different researches. Liu et al. [28] reported the diagnostic performance of prediction for occult peritoneal metastasis in advanced gastric cancer in the primary cohort was better than that in validation cohort. Another study [18] showed that the difference of the diagnostic efficiency AUC of radiomics model was not significant in predicting the malignant potential of GIST between primary cohort and external validation cohort. Our study revealed the differences of diagnostic efficiency AUC between radiomic nomogram and clinical + radiomic feature model in primary cohort and validation cohort were not statistically significant. The results indicated that CT-based radiomic nomogram could accurately predict RM of GST. Moreover, the radiomic nomogram results were not affected by the clinical features and subjective analysis. Some reports revealed the same results in gastrointestinal neoplasms. Sun et al. [15] found from 106 patients with gastric cancer that radiomic nomogram cohort showed a better predicting performance in response to the neoadjuvant chemotherapy than clinical score cohort (based on pre-operative clinical variables), but without significant difference (P = 0.09). By contrast, our results indicated that radiomics model had a higher diagnostic efficiency in predicting the RM of GST, while clinical features had limited value in optimizing the performance. The underlying explanation for our good performance of the radiomic model might be the fact that the internal architecture of lesion heterogeneity reflected by radiomic characteristic was associated with biological behavior and microscopic structure of GST [29, 30], which were criti-

Table 4. The ROC analysis of the clinical and radiomics model

Cohort	Model	Category	Malignant	Benign	Total	Accuracy	Sensitivity	Specificity	AUC
Primary	Radiomics	Malignant	13	34	47				
		Benign	4	114	118	77.0%	76.5%	77.0%	0.816
	Clinical and Radiomics	Malignant	13	34	47				
		Benign	4	114	118	77.0%	76.5%	77.0%	0.833
Validation	Radiomics	Malignant	7	7	14				
		Benign	1	56	57	88.7%	87.5%	88.9%	0.946
	Clinical and Radiomics	Malignant	7	7	14				
		Benign	1	56	57	88.7%	87.5%	88.9%	0.937

Note: DeLong test was used to compare the AUC of radiomic nomogram and clinical + radiomic feature model in primary cohort (P = 0.840) and validation cohort (P = 0.857).

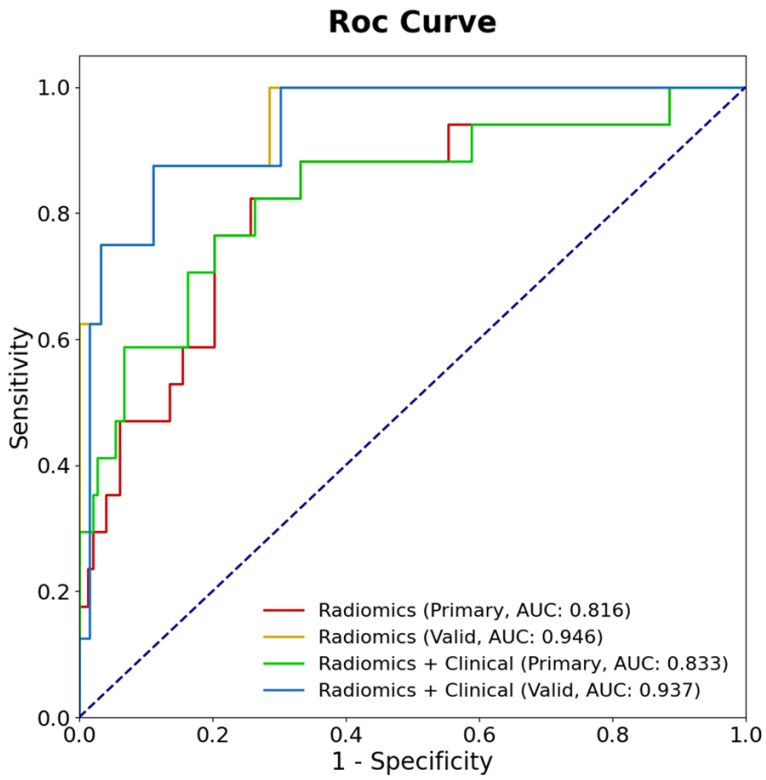

Figure 4. Receiver operating characteristic (ROC) curves of the Radiomics model and the Clinical and Radiomics model in primary and validation cohorts. Area under the curve (AUC) in validation cohorts were significantly higher than primary cohort in predicting RM of GST in the two models. The AUC of radiomics model and clinical + radiomics model in primary cohort and validation cohort had little difference.

cal factors influencing the efficacy in predicting RM of GST.

However, some limitations in this study should be noted. First, the number of recurrence type of GST patients was relatively small, possibly affecting the statistical power. We may need to increase sample size in the future research to improve the accuracy and stability of the predicting radiomic nomogram model. Second, this study lacks external data validation, which is also essential in the future research. Third, our research is based on radiomic and clinical features to predict the RM of GST. Therefore, we need to use a variety of large sample data sets to improve the predicting stability of the RM model in the later research. By improving the performance of the prognostic analysis model, we will build a superior CT-based radiomic nomogram in predicting the RM of GST.

Conclusions

This study investigated the radiomic features extracted from GST. To explore the correlation between the radiomic features and recurrence, metastasis of GST, we constructed a stable and effective model for predicting the prognosis and recurrence of GST. The results of this study indicated that CT-based radiomic nomogram has great potential in non-invasively predicting the RM of GST before operation.

Acknowledgements

This study was supported by Zhejiang Provincial Natural Science Foundation of China (No. LGF21H030004); Medical Health Science and

Technology Project of Zhejiang Province (2019-RC028, 2018KY410).

Disclosure of conflict of interest

None.

Abbreviations

AI, artificial intelligence; AUC, Area Under the Curve; CT, computed tomography; GIST, gastrointestinal stromal tumors; GLCM, wavelet.HHL glcm Maximum Probability; GLSZM, logarithm glszm large area low gray level emphasis; GST, gastric stromal tumors; HU, Hounsfield unit; LASSO, least absolute shrinkage selection operator; MaxDT, maximum diameter of the tumor interface; MDCT, multi-detector computed tomography; MinDT, minimum diameter of the tumor interface; non-RM, non-recurrence/metastasis; NIH, National Institutes of Health; OSS, original shape Sphericity; RM, recurrence and/or metastasis; ROI, regions of interest; Rad-score, radiomics score; ROC, Receiver Operating Characteristic; WLFM, wavelet.LLL firstorder Median.

Address correspondence to: Drs. Jian Wang and Guangzhao Yang, Department of Radiology, Tongde Hospital of Zhejiang Province, No. 234, Gucui Road, Hangzhou 310012, Zhejiang Province, China. E-mail: 119202405@qq.com (JW); 13757118367@163.com (GZY)

References

[1] Burgoyne AM, Somaiah N and Sicklick JK. Gastrointestinal stromal tumors in the setting of multiple tumor syndromes. Curr Opin Oncol 2014; 26: 408-414.

[2] Wei SC, Xu L, Li WH, Li Y, Guo SF, Sun XR and Li WW. Risk stratification in GIST: shape quantification with CT is a predictive factor. Eur Radiol 2020; 30: 1856-1865.

[3] Scola D, Bahoura L, Copelan A, Shirkhoda A and Sokhandon F. Getting the GIST: a pictorial review of the various patterns of presentation of gastrointestinal stromal tumors on imaging. Abdom Radiol (NY) 2017; 42: 1350-1364.

[4] Joensuu H. Risk stratification of patients diagnosed with gastrointestinal stromal tumor. Hum Pathol 2008; 39: 1411-1419.

[5] Zhang L, Kang L, Li G, Zhang X, Ren J, Shi Z, Li J and Yu S. Computed tomography-based radiomics model for discriminating the risk stratification of gastrointestinal stromal tumors. Radiol Med 2020; 125: 465-473.

[6] Eriksson M, Reichardt P, Sundby Hall K, Schütte J, Cameron S, Hohenberger P, Bauer S, Leinonen M, Reichardt A, Rejmyr Davis M, Alvegård T and Joensuu H. Needle biopsy through the abdominal wall for the diagnosis of gastrointestinal stromal tumour - does it increase the risk for tumour cell seeding and recurrence? Eur J Cancer 2016; 59: 128-133.

[7] Mazzei MA, Cioffi Squitieri N, Vindigni C, Guerrini S, Gentili F, Sadotti G, Mercuri P, Righi L, Lucii G, Mazzei FG, Marrelli D and Volterrani L. Gastrointestinal stromal tumors (GIST): a proposal of a "CT-based predictive model of Miettinen index" in predicting the risk of malignancy. Abdom Radiol (NY) 2020; 45: 2989-2996.

[8] Mantese G. Gastrointestinal stromal tumor: epidemiology, diagnosis, and treatment. Curr Opin Gastroenterol 2019; 35: 555-559.

[9] Xu F, Zhu W, Shen Y, Wang J, Xu R, Qutesh C, Song L, Gan Y, Pu C and Hu H. Radiomic-based quantitative CT analysis of pure ground-glass nodules to predict the invasiveness of lung adenocarcinoma. Front Oncol 2020; 10: 872.

[10] Tan JW, Wang L, Chen Y, Xi W, Ji J, Wang L, Xu X, Zou LK, Feng JX, Zhang J and Zhang H. Predicting chemotherapeutic response for far-advanced gastric cancer by radiomics with deep learning semi-automatic segmentation. J Cancer 2020; 11: 7224-7236.

[11] Xu X, Zhang HL, Liu QP, Sun SW, Zhang J, Zhu FP, Yang G, Yan X, Zhang YD and Liu XS. Radiomic analysis of contrast-enhanced CT predicts microvascular invasion and outcome in hepatocellular carcinoma. J Hepatol 2019; 70: 1133-1144.

[12] Li J, Zhang C, Wei J, Zheng P, Zhang H, Xie Y, Bai J, Zhu Z, Zhou K, Liang X, Xie Y and Qin T. Intratumoral and peritumoral radiomics of contrast-enhanced CT for prediction of disease-free survival and chemotherapy response in stage II/III gastric cancer. Front Oncol 2020; 10: 552270.

[13] Dimitrakopoulou-Strauss A, Ronellenfitsch U, Cheng C, Pan L, Sachpekidis C, Hohenberger P and Henzler T. Imaging therapy response of gastrointestinal stromal tumors (GIST) with FDG PET, CT and MRI: a systematic review. Clin Transl Imaging 2017; 5: 183-197.

[14] Scola D, Bahoura L, Copelan A, Shirkhoda A and Sokhandon F. Getting the GIST: a pictorial review of the various patterns of presentation of gastrointestinal stromal tumors on imaging. Abdom Radiol (NY) 2017; 42: 1350-1364.

[15] Sun KY, Hu HT, Chen SL, Ye JN, Li GH, Chen LD, Peng JJ, Feng ST, Yuan YJ, Hou X, Wu H, Li X, Wu TF, Wang W and Xu JB. CT-based radiomics scores predict response to neoadjuvant chemotherapy and survival in patients with gastric cancer. BMC Cancer 2020; 20: 468.

[16] Chen X, Yang Z, Yang J, Liao Y, Pang P, Fan W and Chen X. Radiomics analysis of contrast-enhanced CT predicts lymphovascular invasion and disease outcome in gastric cancer: a preliminary study. Cancer Imaging 2020; 20: 24.
[17] Liu S, He J, Liu S, Ji C, Guan W, Chen L, Guan Y, Yang X and Zhou Z. Radiomics analysis using contrast-enhanced CT for preoperative prediction of occult peritoneal metastasis in advanced gastric cancer. Eur Radiol 2020; 30: 239-246.
[18] Chen T, Ning Z, Xu L, Feng X, Han S, Roth HR, Xiong W, Zhao X, Hu Y, Liu H, Yu J, Zhang Y, Li Y, Xu Y, Mori K and Li G. Radiomics nomogram for predicting the malignant potential of gastrointestinal stromal tumours preoperatively. Eur Radiol 2019; 29: 1074-1082.
[19] Mazzei MA, Cioffi Squitieri N, Vindigni C, Guerrini S, Gentili F, Sadotti G, Mercuri P, Righi L, Lucii G, Mazzei FG, Marrelli D and Volterrani L. Gastrointestinal stromal tumors (GIST): a proposal of a "CT-based predictive model of Miettinen index" in predicting the risk of malignancy. Abdom Radiol (NY) 2020; 45: 2989-2996.
[20] O'Neill AC, Shinagare AB, Kurra V, Tirumani SH, Jagannathan JP, Baheti AD, Hornick JL, George S and Ramaiya NH. Assessment of metastatic risk of gastric GIST based on treatment-naïve CT features. Eur J Surg Oncol 2016; 42: 1222-1228.
[21] Lau S, Tam KF, Kam CK, Lui CY, Siu CW, Lam HS and Mak KL. Imaging of gastrointestinal stromal tumour (GIST). Clin Radiol 2004; 59: 487-498.
[22] Sah BR, Owczarczyk K, Siddique M, Cook GJR and Goh V. Radiomics in esophageal and gastric cancer. Abdom Radiol (NY) 2019; 44: 2048-2058.
[23] Cannella R, La Grutta L, Midiri M and Bartolotta TV. New advances in radiomics of gastrointestinal stromal tumors. World J Gastroenterol 2020; 26: 4729-4738.
[24] Yu MH, Lee JM, Baek JH, Han JK and Choi BI. MRI features of gastrointestinal stromal tumors. AJR Am J Roentgenol 2014; 203: 980-991.
[25] Xu J, Zhou J, Wang X, Fan S, Huang X, Xie X and Yu R. A multi-class scoring system based on CT features for preoperative prediction in gastric gastrointestinal stromal tumors. Am J Cancer Res 2020; 10: 3867-3881.
[26] Zheng T, Du J, Yang L, Dong Y, Wang Z, Liu D, Wu S, Shi Q, Wang X and Liu L. Evaluation of risk classifications for gastrointestinal stromal tumor using multi-parameter Magnetic Resonance analysis. Abdom Radiol (NY) 2021; 46: 1506-1518.
[27] Wang C, Li H, Jiaerken Y, Huang P, Sun L, Dong F, Huang Y, Dong D, Tian J and Zhang M. Building CT radiomics-based models for preoperatively predicting malignant potential and mitotic count of gastrointestinal stromal tumors. Transl Oncol 2019; 12: 1229-1236.
[28] Liu S, He J, Liu S, Ji C, Guan W, Chen L, Guan Y, Yang X and Zhou Z. Radiomics analysis using contrast-enhanced CT for preoperative prediction of occult peritoneal metastasis in advanced gastric cancer. Eur Radiol 2020; 30: 239-246.
[29] O'Connor JP, Aboagye EO, Adams JE, Aerts HJ, Barrington SF, Beer AJ, Boellaard R, Bohndiek SE, Brady M, Brown G, Buckley DL, Chenevert TL, Clarke LP, Collette S, Cook GJ, deSouza NM, Dickson JC, Dive C, Evelhoch JL, Faivre-Finn C, Gallagher FA, Gilbert FJ, Gillies RJ, Goh V, Griffiths JR, Groves AM, Halligan S, Harris AL, Hawkes DJ, Hoekstra OS, Huang EP, Hutton BF, Jackson EF, Jayson GC, Jones A, Koh DM, Lacombe D, Lambin P, Lassau N, Leach MO, Lee TY, Leen EL, Lewis JS, Liu Y, Lythgoe MF, Manoharan P, Maxwell RJ, Miles KA, Morgan B, Morris S, Ng T, Padhani AR, Parker GJ, Partridge M, Pathak AP, Peet AC, Punwani S, Reynolds AR, Robinson SP, Shankar LK, Sharma RA, Soloviev D, Stroobants S, Sullivan DC, Taylor SA, Tofts PS, Tozer GM, van Herk M, Walker-Samuel S, Wason J, Williams KJ, Workman P, Yankeelov TE, Brindle KM, McShane LM, Jackson A and Waterton JC. Imaging biomarker roadmap for cancer studies. Nat Rev Clin Oncol 2017; 14: 169-186.
[30] Liu S, He J, Liu S, Ji C, Guan W, Chen L, Guan Y, Yang X and Zhou Z. Radiomics analysis using contrast-enhanced CT for preoperative prediction of occult peritoneal metastasis in advanced gastric cancer. Eur Radiol 2020; 30: 239-246.